Anal. Chem. **2009,** *81,* 8033–8040

Prefluorescent Nitroxide Probe for the Highly Sensitive Determination of Peroxyl and Other Radical Oxidants

Min Jia,[†] Yu Tang,[†,‡] Yiu-Fai Lam,[†] Sarah A. Green,*[,‡] and Neil V. Blough*[,†]

Department of Chemistry and Biochemistry, University of Maryland, College Park, Maryland 20742, and Chemistry Department, Michigan Technological University, Houghton, Michigan 49931

Fluorescamine derivatized 3-amino-2,2,5,5,-tetramethyl-1-pyrrolidinyloxy (I) is shown to undergo an irreversible reaction with peroxyl radicals and other radical oxidants to generate a more highly fluorescent diamagnetic product (II) and thus can be used as a highly sensitive and versatile probe to determine oxidant production optically, either by monitoring the changes in fluorescence intensity, by HPLC analysis with fluorescence detection, or by a combination of both approaches. By changing the $[O_2]$/[I] ratio, we show that peroxyl radicals can be detected and quantified preferentially in the presence of other radical oxidants. Detection of photochemically produced peroxyl radicals is achieved by employing 3-amino-2,2,5,5,-tetramethyl-1-pyrrolidinyloxy (3-ap) alone, followed by derivatization with fluorescamine. With employment of HPLC analysis, the detection limit of II at a S/N of 2 is ~3 nM for a 125 μL injection. Preliminary applications include the detection of peroxyl radicals generated thermally in soybean phosphatidylcholine liposomes and produced photochemically in tap water.

Peroxyl radicals, formed by the rapid addition of molecular oxygen to carbon-centered radicals, play an important role in many pathological processes, chronic diseases, and aging due to their involvement in the oxidative degradation of DNA and proteins and in the autoxidation of lipids within cell membranes.[1] These species are also key intermediates in thermal and photochemical degradation of both natural and man-made materials.[2]

Although a variety of approaches have been employed to detect peroxyl radicals, including spin trapping with electron paramagnetic resonance (EPR) detection[3] and fluorescence sensors,[4−6] most of these methods suffer from one or more problems such as lack of selectivity, low sensitivity, limited stability, and most importantly, difficulties in quantification.

Since their initial introduction in the late 1980s and early 1990s,[7−11] the use of prefluorescent nitroxide sensors[12] to detect and quantify radical formation has expanded to include a wide range of applications.[13−23] This approach utilizes stable nitroxide radicals as optical switches. By covalently coupling a nitroxide at a short distance from a chromophore, fluorescence emission from the chromophore can be largely quenched.[7,8,24] Upon reaction of the nitroxide moiety with (usually carbon-centered) radicals to form diamagnetic products,[25,26] the intramolecular quenching pathway is eliminated and fluorescence emission is greatly enhanced,[7,8,24] thereby allowing radicals to be detected and quantified, either through changes in

* To whom correspondence should be addressed. Phone, 301 405 0051; fax, 301 314 9121; e-mail, neilb@umd.edu (N. V. Blough). Phone, 906 487 2048; fax, 906 487 2061; e-mail, sgreen@mtu.edu (S. A. Green).

† University of Maryland.

‡ Michigan Technological University.

(1) Halliwell, B.; Gutteridge, J. M. C. *Free Radicals in Biology and Medicine*, 4th ed.; Oxford University Press: Oxford, U.K., 2007.

(2) Micallef, A. S.; Blinco, J. P.; George, G. A.; Reid, D. A.; Rizzardo, E.; Huang, S. H.; Bottle, S. E. *Polym. Degrad. Stab.* **2005**, *89*, 427–435.

(3) Jones, C. M.; Burkitt, M. J. *J. Chem. Soc., Perkin Trans. 2* **2002**, 2044–2051.

(4) DeLange, R. J.; Glazer, A. N. *Anal. Biochem.* **1989**, *177*, 300–306.

(5) Maulik, G.; Salgia, R.; Makrigiorgos, G. M. *Methods Enzymol.* **2002**, *352*, 80–91.

(6) Heyne, B.; Beddie, C.; Scaiano, J. C. *Org. Biomol. Chem.* **2007**, *5*, 1454–1458.

(7) Blough, N. V.; Simpson, D. J. *J. Am. Chem. Soc.* **1988**, *110*, 1915–1917.

(8) Green, S. A.; Simpson, D. J.; Zhou, G.; Ho, P. S.; Blough, N. V. *J. Am. Chem. Soc.* **1990**, *112*, 7337–7346.

(9) Kieber, D. J.; Blough, N. V. *Anal. Chem.* **1990**, *62*, 2275–2283.

(10) Kieber, D. J.; Blough, N. V. *Free Radical Res. Commun.* **1990**, *10*, 109–117.

(11) Gerlock, J. L.; Zacmanidis, P. L.; Bauer, D. R.; Simpson, D. J.; Blough, N. V.; Salmeen, I. T. *Free Rad. Res. Commun.* **1990**, *10*, 119–121.

(12) A term originally coined by Scaiano and co-workers and employed herein: Ballesteros, O. G.; Maretti, L.; Sastre, R.; Scaiano, J. C. *Macromolecules* **2001**, *34*, 6184–6187.

(13) Zhu, Q.; Lian, Y.; Thyagarajan, S.; Rokita, S. E.; Karlin, K. D.; Blough, N. V. *J. Am. Chem. Soc.* **2008**, *130*, 6304–6305.

(14) Gan, D.; Jia, M.; Vaughan, P. P.; Falvey, D. E.; Blough, N. V. *J. Phys. Chem. A* **2008**, *112*, 2803–2812.

(15) Alaghmand, M.; Blough, N. V. *Environ. Sci. Technol.* **2007**, *41*, 2364–2370.

(16) Fairfull-Smith, K. E.; Blinco, J. P.; Keddie, D. J.; George, G. A.; Bottle, S. E. *Macromolecules* **2008**, *41*, 1577–1580.

(17) Coenjarts, C.; Garcia, O.; Llauger, L.; Palfreyman, J.; Vinette, A. L.; Scaiano, J. C. *J. Am. Chem. Soc.* **2003**, *125*, 620–621.

(18) Aliaga, C.; Juarez-Ruiz, J. M.; Scaiano, J. C.; Aspee, A. *Org. Lett.* **2008**, *10*, 2147–2150.

(19) Flicker, T. M.; Green, S. A. *Environ. Health Perspect.* **2001**, *109*, 765–771.

(20) Chen, W.; Wang, X.; Tu, X.; Pei, D.; Zhao, Y.; Guo, X. *Small* **2008**, *6*, 759–764.

(21) Kalai, T.; Schindler, J.; Balog, M.; Fogassy, E.; Hideg, K. *Tetrahedron* **2008**, *64*, 1094–1100.

(22) Borisenko, G. G.; Martin, I.; Zhao, Q.; Amoscato, A. A.; Kagan, V. E. *J. Am. Chem. Soc.* **2004**, *126*, 9221–9232.

(23) Fairfull-Smith, K. E.; Bottle, S. E. *Eur. J. Org. Chem.* **2008**, *32*, 5391–5400.

(24) Herbelin, S. E.; Blough, N. V. *J. Phys. Chem. B* **1998**, *102*, 8170–8176.

(25) Ingold, K. U. In *Landolt-Bornstein Numerical Data and Functional Relationships in Science and Technology, Subvolume C, Radical Reaction Rates in Liquids*; Fischer, H., Ed.; Springer-Verlag: New York, 1983; Vol. 13, pp 166–270.

(26) Beckwith, A. L. J.; Bowry, V. W.; Ingold, K. U. *J. Am. Chem. Soc.* **1992**, *114*, 4983–4992.

10.1021/ac901374m CCC: $40.75
Published on Web 09/11/2009

Scheme 1. Reaction of I with Carbon-Centered Radicals to Form the Alkoxylamine Product under Anaerobic Conditions and with Peroxyl Radicals to Form II under Aerobic Conditions

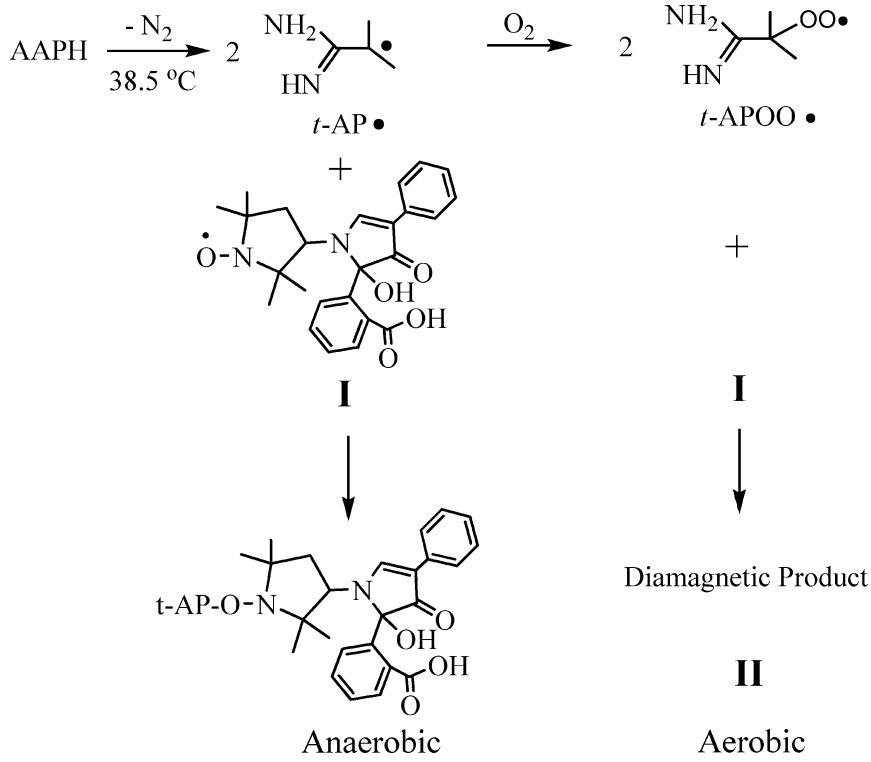

fluorescence intensity[7,11,12,17,18] or through product analysis by high-performance liquid chromatography (HPLC)[9,27−31] or liquid chromatography/mass spectrometry (LC/MS).[32,33]

Here we demonstrate that the prefluorescent nitroxide probe, **I** (Scheme 1), synthesized by reaction of 3-amino-2,2,5,5,-tetramethyl-1-pyrrolidinyloxy (3-ap) with fluorescamine,[27,28] undergoes a unique, irreversible reaction with peroxyl radicals to form a more highly fluorescing diamagnetic product (**II**) and thus can be employed to detect and quantify peroxyl radicals optically. Although other one-electron (radical) oxidants such as $^{\bullet}NO_2$ and $CO_3^{\bullet-}$ are also shown to react with **I** to form **II**, we demonstrate that peroxyl radicals can be preferentially detected in their presence by changing the $[O_2]/[\mathbf{I}]$ ratio (Scheme 1).

In this article, the stoichiometry of the peroxyl radical reaction with **I** is first established and is shown to differ from that of other amino-nitroxides. The use of **I** to determine the formation rate of peroxyl radicals by thermolysis and radiolysis of simple model systems is shown, with this approach then employed to determine the production of peroxyl radicals in an aqueous dispersion of soybean phosphatidylcholine (PC) liposomes. Finally, 3-ap alone is used to determine peroxyl radicals generated photochemically from tap water following derivatization of its product with fluorescamine and subsequent chromatographic analysis.

EXPERIMENTAL SECTION

Chemicals. Nitroxides (3-ap, 3-aminomethyl-2,2,5,5-tetramethyl-1-pyrrolydinyloxy (3-amp), 3-carbamoyl-2,2,5,5-tetramethyl-1-pyrrolidineoxy (3-cp), and 4-amino-2,2,6,6-tetramethylpiperidinyloxy (4-at)) and fluorescamine were purchased from Acros and Sigma Aldrich, respectively. 2,2′-Azo-bis-(2-amidinopropane) dihydrochloride (AAPH) and azobisisobutyronitrile (AIBN) were purchased from Cyman Chemical Co. Sodium phosphate (99.999%) and sodium hydroxide were obtained from Aldrich. DMSO, HPLC grade methanol, acetonitrile, and glacial acetic acid were all purchased from Fisher. Refined lecithin was purchased from Alfa Aesar. All chemicals were used without further purification. Pure water for all experiments was obtained from a Millipore Milli-Q system.

Thermolysis. Thermolysis of AAPH was carried out in a 4 mL quartz cuvette in pH 7.4, 50 mM sodium phosphate buffer in a thermostatted water bath at 38.5 ± 0.5 °C. The stock AAPH solution (80 mM) was prepared daily and stored in an ice bath prior to thermolysis. Reactions were initiated by immersion of the reaction vessel in the water bath. Reactions were terminated by placing aliquots of the reaction mixture in a −20 °C freezer for minimally 10 min. For anaerobic experiments, samples were purged for 20 min with N_2, with the headspace of the cuvette continuously purged with N_2 during thermolysis. The liposome preparation procedure has been reported previously.[34−36] Briefly, 1 mg of AIBN and 375 mg of lecithin were dissolved in 5

(27) Li, B.; Gutierrez, P. L.; Blough, N. V. *Anal. Chem.* **1997**, *69*, 4295–4302.
(28) Li, B.; Gutierrez, P. L.; Blough, N. V. *Methods Enzymol.* **1999**, *300*, 202–216.
(29) Li, B.; Gutierrez, P. L.; Amstad, P.; Blough, N. V. *Chem. Res. Toxicol.* **1999**, *12*, 1042–1049.
(30) Thomas-Smith, T. E.; Blough, N. V. *Environ. Sci. Technol.* **2001**, *35*, 2721–2726.
(31) Vaughan, P. P.; Blough, N. V. *Environ. Sci. Technol.* **1998**, *32*, 2947–2953.
(32) Johnson, C. G.; Caron, S.; Blough, N. V. *Anal. Chem.* **1996**, *68*, 867–872.
(33) Kieber, D. J.; Johnson, C. G.; Blough, N. V. *Free Radical Res. Commun.* **1992**, *16*, 35–39.
(34) Yamamoto, Y.; Niki, E.; Kamiya, Y. *Lipids* **1982**, *17*, 870–877.
(35) Yamamoto, Y.; Niki, E.; Kamiya, Y.; Shimasaki, H. *Biochim. Biophys. Acta* **1984**, 332–340.
(36) Takahashi, M.; Tsuchiya, J.; Niki, E. *J. Am. Chem. Soc.* **1989**, *111*, 6350–6353.
(37) Notre Dame Radiation Chemistry Data Center. http://www.rcdc.nd.edu/Solnkin2/.

mL of chloroform, with the solvent then evaporated to produce a thin film. **I** (28.4 μM) dissolved in 5 mL of 0.1 M NaCl solution was added to obtain a milky liposome suspension. This suspension was promptly placed into a 50 ± 1 °C water bath under an atmospheric of oxygen to initiate the reaction. The reaction was terminated in the same way as in AAPH experiments. The suspensions were filtered through a 0.2 μm Puradisc filter before injection into an HPLC column.

Steady State Radiolysis. Steady state radiolysis was performed using a ^{60}Co source at room temperature. The dose rate was determined in each experiment using a Fricke dosimeter. DMSO (20 mM) in 10 mM pH 7.4 phosphate buffer was saturated either with N_2O alone or with 80% N_2O/20% O_2 in a Wheaton 5 mL serum vial. The vials were immediately sealed (while still purging) with Wheaton rubber plug stoppers, which were then fastened by an aluminum crimping tool. $CO_3^{\bullet-}$ and $^{\bullet}NO_2$ were produced by γ irradiation of N_2O saturated, 100 mM Na_2CO_3 solution, or 10 mM $NaNO_2$ solution in 5 mM phosphate buffer (pH 7.4), respectively. The generation of these radicals and their possible subsequent reactions are provided below:

$$H_2O \rightarrow {}^{\bullet}OH + e_{aq}^{-} + H_3O^{+} + {}^{\bullet}H + OH^{-} + H_2 + H_2O_2 \quad (1)$$

$$e_{aq}^{-} + N_2O + H_2O \xrightarrow{k_2 = 9.1\times10^9\ M^{-1}s^{-1}} {}^{\bullet}OH + OH^{-} + N_2 \quad (2)$$

$$\bullet OH + \underset{CH_3}{\overset{CH_3}{\diagdown}}S{=}O \xrightarrow{k_3 = 6.6\times10^9\ M^{-1}s^{-1}} \bullet CH_3 + H_3C{-}\overset{O}{\overset{\|}{S}}{-}OH \quad (3)$$

$$^{\bullet}OH + NO_2^{-} \xrightarrow{k_4 = 6.0\times10^9\ M^{-1}s^{-1}} {}^{\bullet}NO_2 + OH^{-} \quad (4)$$

$$^{\bullet}OH + CO_3^{2-} \xrightarrow{k_5 = 3.9\times10^8\ M^{-1}s^{-1}} CO_3^{\bullet-} + OH^{-} \quad (5)$$

$$^{\bullet}CH_3 + O_2 \xrightarrow{k_6 = 1.6\times10^9\ M^{-1}s^{-1}} CH_3OO^{\bullet} \quad (6)$$

$\bullet CH_3 + \mathbf{I} \xrightarrow{k_7 = 7.8\times10^8\ M^{-1}s^{-1}}$ 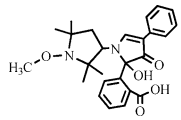 **VI** (7)

$$CH_3OO^{\bullet} + \mathbf{I} \xrightarrow{k_8 = 10^6-10^7\ M^{-1}s^{-1}\ (ref\ 39)} \mathbf{II} \quad (8)$$

$$^{\bullet}NO_2 + \mathbf{I} \xrightarrow{k_9 = 10^8\ M^{-1}s^{-1}\ (ref\ 40)} \mathbf{II} \quad (9)$$

$$CO_3^{\bullet-} + \mathbf{I} \xrightarrow{k_{10} = 10^8\ M^{-1}s^{-1}\ (ref\ 44)} \mathbf{II} \quad (10)$$

Photolysis. Samples were placed in a 1 cm cuvette and irradiated with a 300 W xenon lamp. The actinic light was first filtered through 22 cm of Milli Q water and then through a 275 nm long pass filter to provide a light intensity of 150 mW/cm^2.

HPLC. The reversed-phase HPLC system has been described previously.[27,28] A 4 μm RP C18 packing Nova-Pack column in a RCM 8 cm × 10 cm Waters radial compression module was employed for separation. In most cases, the mobile phase was 65% sodium acetate buffer (50 mM, pH 4.0) and 35% methanol (v/v) with a flow rate of 1.0 mL/min. The temperature of the column was maintained at 29 °C. The fluorescence detector was a Hitachi model L4870 set at 390 nm (excitation) and 490 nm (emission). A 125 μL sample loop was employed.

Fluorometer. Emission spectra were collected with an SLM-Aminco AB2 spectrofluorometer. Wavelengths were set at 390 nm (excitation) and 400−700 nm (emission) with 4 nm bandpasses on both the excitation and emission monochromators. Fluorescence quantum yields were measured as described previously.[24]

Electron Paramagnetic Resonance. A Bruker ESP300E EPR spectrometer was used to follow the nitroxide spin loss. Samples were drawn into 50 μL capillary tubes, sealed top and bottom with Critoseal, and placed within standard 3 mm i.d. quartz EPR tubes. Standard instrument settings were frequency 9.8 GHz; microwave power 9.4 mW; modulation amplitude 1.0 G. Spin levels were determined from areas obtained by double integration of the EPR spectra, as compared with known concentrations of 3-cp.

Cyclic Voltammetry. Cyclic voltammetry of the nitroxides was performed using a homemade three-electrode cell on a CHI660A workstation. The scan range was 0−1.0 V vs Ag/AgCl reference electrode, and the scan rate was 100 mV/s. Both the working and counter electrodes were platinum wire. Nitroxides were dissolved in pH 7.4, 50 mM sodium phosphate buffer saturated with K_2SO_4.

Synthesis and Purification of Products. Synthesis of **I** and of fluorescamine-derivatized 3-amp and 4-at have been described previously.[24,27,28] Bulk electrolysis of ~2 mM 3-ap, 3-amp, and 4-at was performed with a three-electrode system on a BAS CV-50W voltammetric analyzer in neutral pH buffer saturated with K_2SO_4. The voltage was 750 mV vs Ag/AgCl, and the electrolysis time was 90 min. A 10 mM fluorescamine solution in acetonitrile was added to the reaction mixture in a 1 mL centrifuge tube and vortexed for 1 min at room temperature. The pH of the solution was adjusted to 8.1, and fluorescamine was added in 5−10-fold molar excess relative to the product. **II** was then separated and purified by HPLC and then extracted in chloroform. **II** was dried under N_2 flow and stored in the freezer at −20 °C until use. Reaction of the 3-ap oxidation product with benzoyl chloride was carried out in aqueous solution. Briefly, 18 mg of 3-ap was oxidized either electrochemically or by t-APOO radical in 10 mL of aqueous solution in a 25 mL conical flask. A total of 800 mg of sodium bicarbonate was added while stirring. Benzoyl chloride (24 mg) was added into the solution, and the mixture was stirred for 20 min. A volume of 20 mL of chloroform was used to extract the product. The solvent was evaporated, and the dry product was redissoved in 3 mL of 50%/50% by volume methanol/water. The product was purified by RP HPLC (mobile phase, 75% H_2O/25% methanol), extracted into chloroform, and dried under N_2. The dry product was stored at −20 °C until further use.

Product Analysis by NMR and Mass Spectrometry. ^{1}H, ^{13}C NMR and COSY, HMBC, HSQC, NOESY, and H2BC were performed on Bruker 500 and 600 MHz spectrometers. Samples were prepared in deuterated chloroform at room temperature.

A linear quadrupole-ion trap (LTQ) Fourier-transform ion cyclotron resonance (FTICR) mass spectrometer at the Woods Hole Oceanographic Institution was employed for high-resolution mass spectral measurements. The ESI spray voltage was 4.3 kV for positive mode and 4.0 kV for negative mode. The capillary temperature was 250 °C. A JEOL AccuTOF-CS ESI-time-of flight (TOF) mass spectrometer at the University of Maryland was also employed in product analysis.

RESULTS

Reaction Stoichiometry. Alkyl radicals (t-AP$^\bullet$) were produced by thermolysis of AAPH under anaerobic conditions (Scheme 1). Under aerobic conditions, these alkyl radicals were converted quantitatively to peroxyl radicals (t-APOO$^\bullet$; ~95%), owing to the high [O_2]/[**I**] ratios employed (varying from ~5 to 20), as well as to the higher reaction rates of carbon-centered radicals with O_2 ($\sim 2-4 \times 10^9$ M^{-1} s^{-1})[38] as compared with the nitroxides ($\sim 1-8 \times 10^8$ M^{-1} s^{-1}).[25,26] EPR was then used to follow the spin loss of **I** under anaerobic and aerobic conditions to compare the reactivity of **I** with t-AP$^\bullet$ and t-APOO$^\bullet$, respectively (Scheme 1; a representative example of EPR spectra is provided in Figure S1 in the Supporting Information).

Identical rates of spin loss were observed for **I** under N_2 and air during the thermolysis of AAPH (Figure 1A), demonstrating that t-APOO$^\bullet$ reacted with **I** to the same extent as t-AP$^\bullet$. Further, the rates were independent of [**I**], indicating that both t-AP$^\bullet$ (under N_2) and t-APOO$^\bullet$ (under air) were reacting quantitatively with **I**. Identical rates of loss were also observed in the reaction of **I** with $CH_3^\bullet$ and $CH_3OO^\bullet$ radicals generated by steady-state radiolysis in the absence and presence of 20% O_2, respectively (Figure 1B), showing that this reaction is not unique to t-APOO$^\bullet$. At the temperatures employed in this study, nitroxides are known to react irreversibly with carbon-centered radicals to produce stable alkoxylamine products.[7−11,25,26] Thus, the identical rates of loss in the presence and absence of O_2 and with increasing [**I**] demonstrates that **I** also reacts irreversibly with peroxyl radicals.

Reaction of **I** with t-APOO$^\bullet$ and $CH_3OO^\bullet$ also led to a dramatic increase in the steady-state fluorescence intensity (Figure 2 and Figure S2 in the Supporting Information), which exhibited a linear relationship with the loss of **I** as determined by EPR (Figure 2 inset and Figure S2 inset in the Supporting Information). Fluorescence quantum yields of HPLC-purified **II** (see below) in H_2O (0.045) and in pH 7.4, 50 mM phosphate buffer (0.041) were about 90-fold higher than that obtained previously for **I** (0.00046)[24] and only about 2-fold lower than that obtained previously for an alkoxyamine adduct of **I** (0.097).[24]

HPLC analysis employing fluorescence detection showed that reaction of either t-APOO$^\bullet$ or $CH_3OO^\bullet$ with **I** produced a single product (**II**) that was not formed under anaerobic conditions (Figure 3 and Figure S3 in the Supporting Information). The fluorescence peak area of **II** increased linearly with the loss of **I** as determined by EPR (Figure 3, inset). This same product was also generated either by the electrochemical oxidation of 3-ap (see below) or by 3-ap reaction with peroxyl radicals when followed immediately by derivatization with fluorescamine at pH 8.1 (Figure S4 in the Supporting Information). **II** was also formed by the reaction of **I** with $^\bullet NO_2$ and $CO_3^{\bullet-}$ radicals generated radiolytically (Figure S5 in the Supporting Information). Prior work has shown that nitroxides react with peroxyl,[39] $^\bullet NO_2$,[40] and $CO_3^{\bullet-}$ [44]

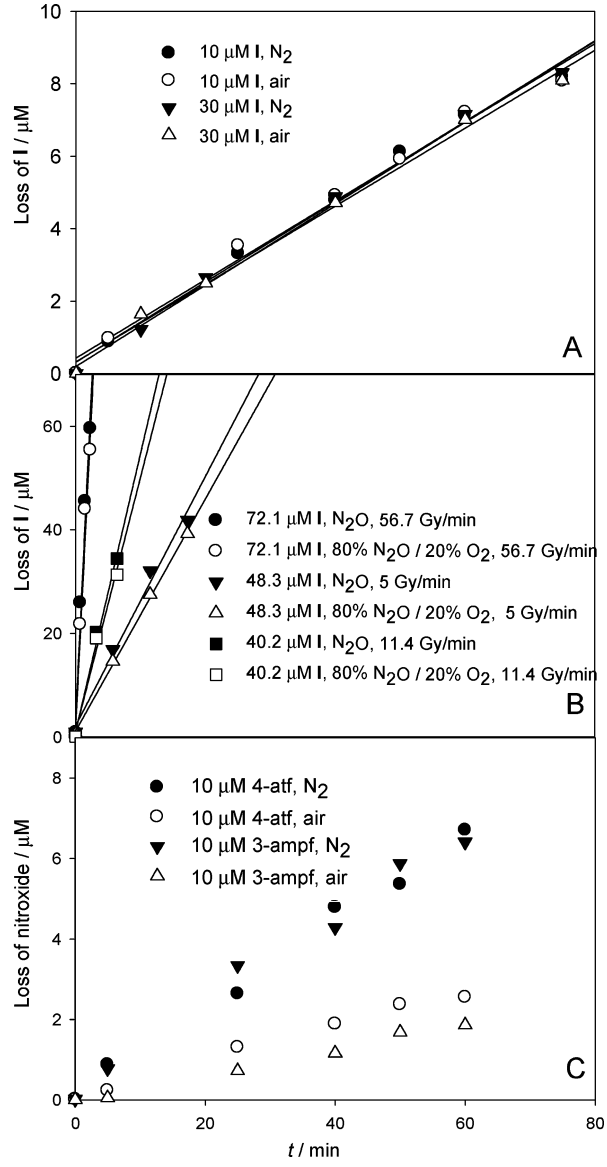

Figure 1. Reaction of nitroxides with peroxyl radicals. (Panel A) Time course for the reaction of **I** with t-AP$^\bullet$ (under N_2) and t-APOO$^\bullet$ (under air) generated by thermolysis of AAPH (1 mM) in 50 mM phosphate buffer, pH 7.4 at 38.5 ± 0.5 °C. [O_2] = 210 μM at this temperature. (Panel B) Time course for the reaction of **I** with $CH_3^\bullet$ (under N_2O) and $CH_3OO^\bullet$ (80% N_2O/20% O_2) generated by γ radiolysis in 10 mM phosphate buffer, pH 7.4 containing [DMSO] = 20 mM, [O_2] = 250 μM. (Panel C) Time course for the reaction of fluorescamine derivatized 4-at (4-atf) and fluorescamine derivatized 3-amp (3-ampf) with t-AP$^\bullet$ (under N_2) and t-APOO$^\bullet$ (under air) in 50 mM phosphate buffer, pH 7.4. [4-atf] or [3-ampf] = 10 μM. Other reaction conditions are the same as in Panel A.

(38) Maillard, B.; Ingold, K. U.; Scaiano, J. C. *J. Am. Chem. Soc.* **1983**, *105*, 5095–5099.

(39) Goldstein, S.; Samuni, A. *J. Phys. Chem. A* **2007**, *111*, 1066–1072.

(40) Goldstein, S.; Samuni, A.; Russo, A. *J. Am. Chem. Soc.* **2003**, *125*, 8364–8370.

(41) Goldstein, S.; Merinyi, G.; Russo, A.; Samuni, A. *J. Am. Chem. Soc.* **2003**, *125*, 789–795.

(42) Samuni, A.; Goldstein, S.; Russo, A.; Mitchell, J.; Krishna, M.; Neta, P. *J. Am. Chem. Soc.* **2002**, *124*, 8719–8724.

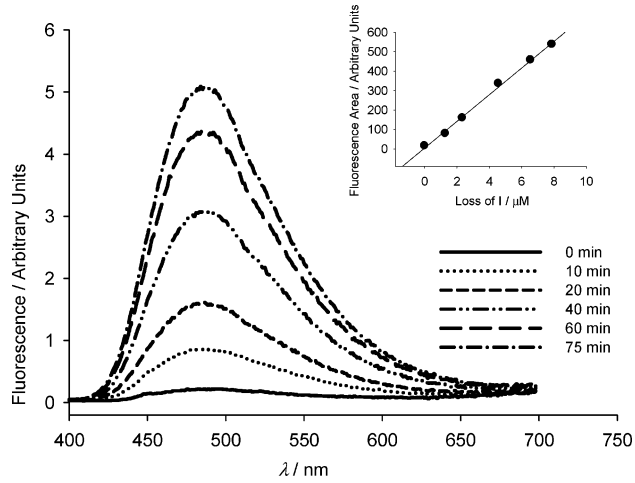

Figure 2. Fluorescence emission spectra of **II** formed by reaction of **I** with t-APOO• produced by thermolysis of AAPH (1 mM) at 38.5 ± 0.5 °C in 50 mM phosphate buffer, pH 7.4. $[O_2] = 210\ \mu M$ and [**I**] = 10 μM. Excitation wavelength was at 386 nm. Inset: Dependence of fluorescence area on the loss of **I** as determined by EPR.

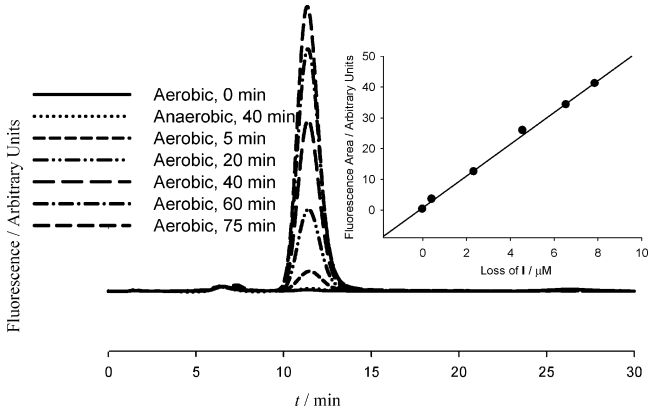

Figure 3. Reversed phase HPLC chromatograms showing the formation of **II** upon reaction of I with t-APOO• produced by thermolysis of AAPH (1 mM) at 38.5 ± 0.5 °C in 50 mM phosphate buffer, pH 7.4. $[O_2] = 210\ \mu M$ and [**I**] = 10 μM. The HPLC mobile phase was 65% sodium acetate buffer/35% MeOH v/v. Excitation wavelength 390 nm, emission wavelength 490 nm. Injection volume was 125 μL. Inset: Dependence of fluorescence peak area on the loss of **I** as determined by EPR.

radicals to initially form the oxoammonium cation (Scheme 2). However, **II** was stable in aqueous solution at room temperature for at least 12 h, both in the absence and presence of NADH,[39−42] illustrating that **II** was not the oxoammonium cation. Further, the 1:1 stoichiometric reaction of this amino-nitroxide (3-ap) with peroxyl radicals (Figure 1) was unique; other fluorescamine-derivatized amino-nitroxides (3-amp and 4-at) exhibited much lower rates of spin loss in the presence of air than in its absence (Figure 1C). For these nitroxides, the lower rates of spin loss in air presumably result from the reversible regeneration of the nitroxyl moiety via the reduction by solution constituents of the oxoammonium cation.[39−42] Unlike both 4-at and 3-amp, 3-ap exhibited an irreversible oxidative wave in its cyclic voltammogram (Figure 4), clearly revealing that the oxoammonium cation of 3-ap is far less stable than that of 4-at and 3-amp and reacts rapidly to form a secondary product. Increasing the scan rate from 100 to 500 mV/s did not lead to the appearance of a reductive wave in the cyclic voltammogram, further indicating that the lifetime of this oxoammonium cation must be very short, under roughly one second, and thus that it is much less likely to be intercepted by solution reductants as is demonstrated by the results in Figure 1.

Product Analysis. Analysis by AccuTOF ESI-MS of the electrochemical oxidation product of 3-ap revealed two major peaks at 157.134 and 118.083 after extraction with chloroform at pH 9 but only one major peak (m/z 118.083) after extraction at pH 12 (Figure S6 in the Supporting Information). We further observed that the initial 3-ap oxidation product, as detected chromatographically following fluorescamine derivatization to form **II**, was not completely stable in aqueous solution but very slowly converted to a more polar, less fluorescent species as the time between formation and derivatization was increased (Figure S7 in the Supporting Information). Ultrahigh resolution FTICR mass spectrometry of the products of 3-ap extracted at pH 9 provided the molecular formula of these two species, $C_8H_{17}N_2O$ (M + H, 157.133 47) and $C_5H_{12}NO_2$ (M + H, 118.086 20). These results suggest that the oxoammonium cation of 3-ap first undergoes rapid ring cleavage and proton loss to form an initial product, either **IIIa** or **IIIb** (M + H, 157.133 47) (Scheme 2), which subsequently converts at higher pH to a secondary product in the absence of derivatization with fluorescamine; this product was tentatively identified as **IV** (M + H: 118.086 20, $C_5H_{12}NO_2$; see Scheme 2 and below).

In contrast, **II**, characterized by FTICR MS following HPLC purification of the fluorescamine-derivatized electrochemical oxidation product of 3-ap, showed no evidence of either of these two structures. Instead, dominant peaks at m/z 395.160 13 and 393.145 64 were observed in positive and negative ion mode, respectively (Figure S8 in the Supporting Information), corresponding to a molecular formula of $C_{22}H_{22}N_2O_5$ (predicted masses: 395.160 15 in positive ion mode and 393.145 60 in negative ion mode). Because the absorption and fluorescence spectra of **II** were identical to that of the alkoxylamine adducts of **I** (Scheme 1, Figure 2), we concluded that the fluorescamine moiety within **II** must be structurally intact. On this basis, **II** was tentatively identified as the structure shown in Scheme 2. Because **II** was also formed following reaction of **I** with peroxyl radicals (Figure 3 and Figure S3 in the Supporting Information) and NO_2 and CO_3^- radicals (Figure S5 in the Supporting Information), **III′** (a or b) is also a likely intermediate in the formation of **II** (Scheme 2). Unfortunately, **II** was not sufficiently stable in organic solvents over the time frame needed to obtain an unequivocal identification by NMR.

In an attempt to resolve this issue, the electrochemical oxidation product of 3-ap was reacted with benzoyl chloride at pH 8.5 to form the stable amide (Scheme 2). Following HPLC purification, this product was identified as the cyclic peroxide **V** (Scheme 2) as established by FTICR MS (Figure S9 in the Supporting Information) and extensive NMR analyses (Figure S10−S23 in the Supporting Information). Although this assignment is consistent with the secondary product **IV** observed by MS following oxidation of 3-ap (Figure S6 in the Supporting

(43) Krishina, M. C.; Grahame, D. A.; Samuni, A.; Mitchell, J. B.; Russo, A. *Proc. Natl. Acad. Sci. U.S.A.* **1992**, *89*, 5537–5541.
(44) Goldstein, S.; Samuni, A.; Hideg, K.; Merinyi, G. *J. Phys. Chem. A* **2006**, *110*, 3679–3685.

Scheme 2. Proposed Reaction Pathways for the Oxoammonium Cation of 3-ap and I

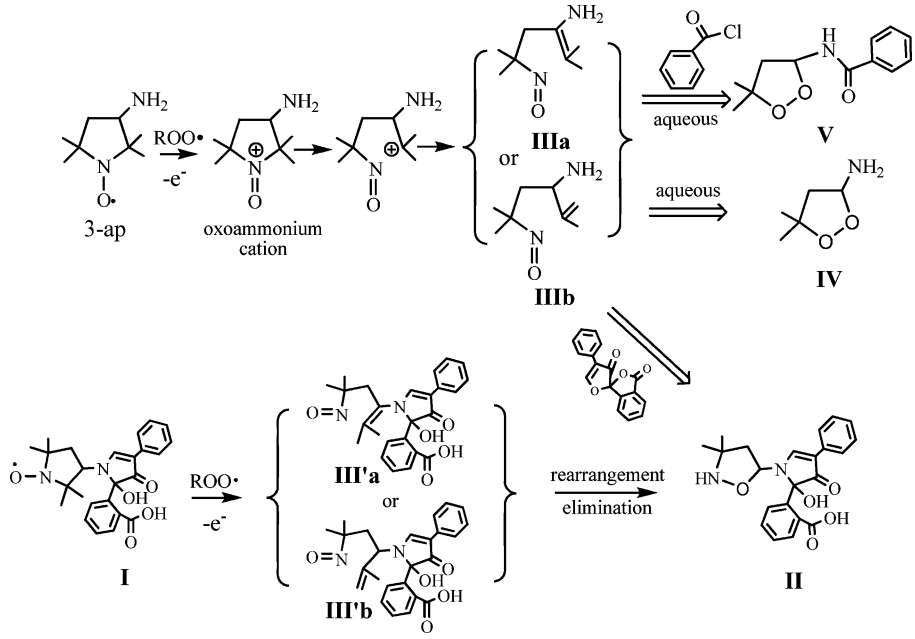

Information and Scheme 2), the subsequent reactions by which this product forms is unclear. Similarly, the secondary reactions by which **II** forms is not obvious, although this product clearly differs from **IV**, suggesting that the presence of the fluorescamine moiety alters the reaction pathway from **III** (and **III′**) to produce **II** (Scheme 2 and Figure S4A,C,D in the Supporting Information). Regardless, the observation that **I** (and 3-ap) undergoes irreversible reaction with peroxyl radicals while most other nitroxides do not[39] can be attributed to the amine moiety at the β-position, which we suggest facilitates the rapid initial ring cleavage and proton loss (Scheme 2).

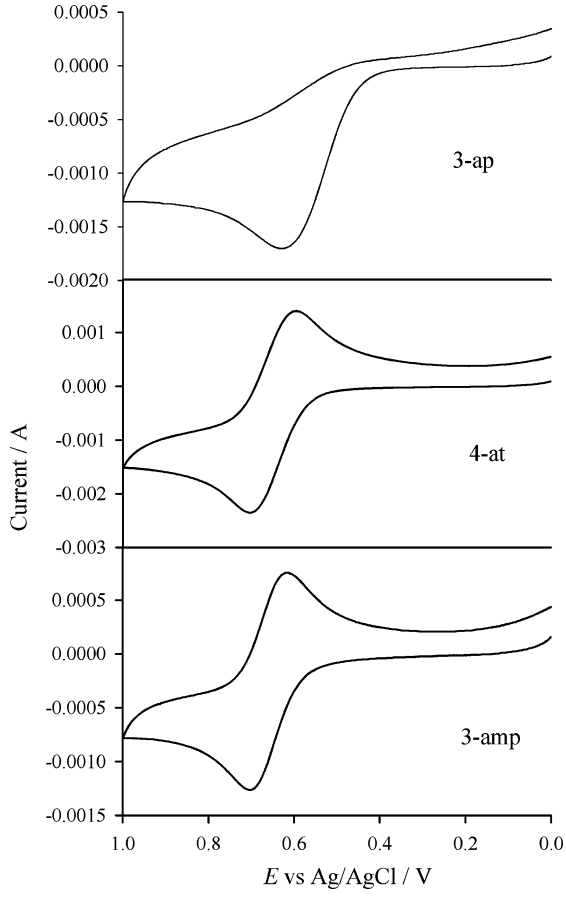

Figure 4. Cyclic voltammetry of nitroxides in K_2SO_4-saturated phosphate buffer (50 mM, pH 7.4). Nitroxide concentrations were 2.5−5 mM. Electrodes: platinum (working and auxiliary) and Ag/AgCl (reference). The scan rate was 100 mV/s, and the scan range was 0−1000 mV.

Selectivity. Our results indicate that other radicals capable of oxidizing **I** to the oxoammonium cation will also generate **II** (Figure S5 in the Supporting Information) and thus will also be detected. In addition to $^{\bullet}NO_2$ and $CO_3^{\bullet-}$, such radicals include the hydroxyl ($^{\bullet}OH$),,[42] alkoxyl ($RO^{\bullet}$), and possibly superoxide ($O_2^{\bullet-}$).[43,44] Radiolytically produced $O_2^{\bullet-}$, however, did not react with **I** to form **II** even under high fluxes of this radical (8 μM/min), consistent with our prior results[27,28] and the fact that the rate constants for reaction of superoxide with pyrrolidinyl nitroxides are 2−3 orders of magnitude lower[43,44] than those for peroxyl radicals[39−41] at neutral to alkaline pH.

Indeed, because published rate constants for reaction of pyrrolidinyl nitroxides with peroxyl radicals are reasonably large ($\sim 10^6-10^7$ M^{-1} s^{-1}),[39] the use of low concentrations of **I** (<40−50 μM) should allow quantitative reaction with peroxyl radicals (e.g., Figures 1A,C, 2, and 3 and Figure S3 in the Supporting Information), while largely precluding interferences from more highly reactive oxidants such as $^{\bullet}OH$ and $RO^{\bullet}$, which under most circumstances will react preferentially with other solution constituents at higher concentrations. Nevertheless, this may not be the case when more selective oxidants such as $^{\bullet}NO_2$ and $CO_3^{\bullet-}$ are also present. Because these other oxidants are not O_2-reactive, while the formation of peroxyl radicals is O_2-dependent, the presence of oxidants other than peroxyl radicals should be readily identified by decreasing the $[O_2]/[\mathbf{I}]$ ratio (Scheme 1); a decrease in the yield of **II**, combined with a concomitant increase in alkoxylamine products, would be

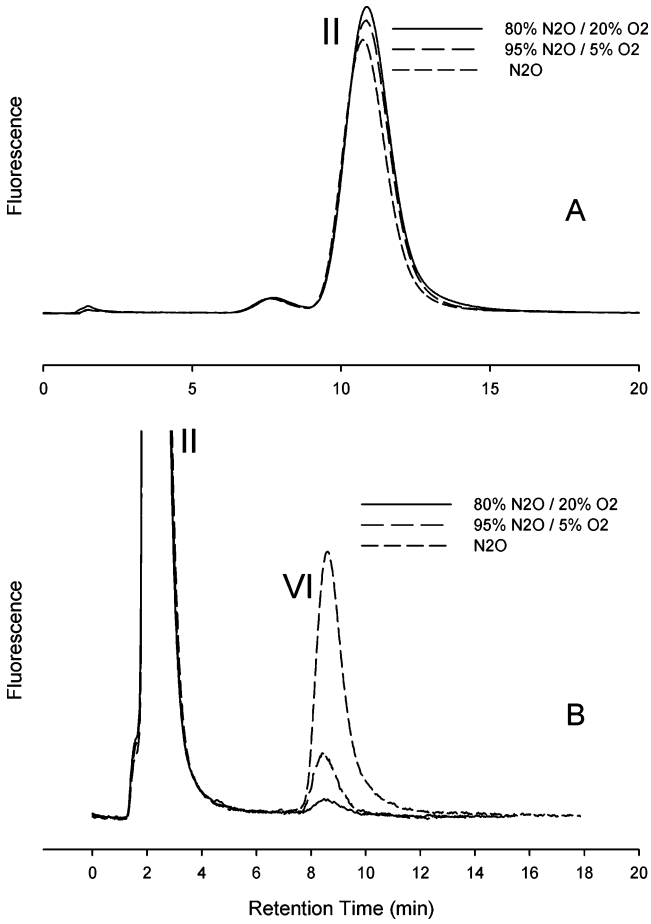

Figure 5. Determination of peroxyl radicals in the presence of $^{\bullet}NO_2$ by γ radiolysis of a solution containing 30 μM **I**, 1.5 mM DMSO, and 20 mM $NaNO_2$. (Panel A) Decrease of **II** formation with decreasing $[O_2]/[\mathbf{I}]$ ratio. HPLC conditions were as in Figure 3. (Panel B) Increase of methoxylamine product (**VI**) with decreasing $[O_2]/[\mathbf{I}]$ ratio. Mobile phase was 60% MeOH and 40% pH 4.0 acetate buffer. Other HPLC conditions are as in Figure 3.

predicted when peroxyl radicals contribute significantly to the total oxidant pool (Scheme 1).

To test this idea, solutions containing 1.5 mM DMSO, 20 mM $NaNO_2$, and N_2O/O_2 ratios ranging from pure N_2O to 80% N_2O/20% O_2 were subjected to γ radiolysis in the presence of 30 μM **I** (Figure 5, see reactions 1−9). Because of the high N_2O concentrations employed, all e^-(aq) is converted quantitatively to $^{\bullet}OH$ under all conditions (reactions 1 and 2). $^{\bullet}OH$ then reacts competitively with DMSO and NO_2^- to form $^{\bullet}CH_3$ and $^{\bullet}NO_2$ radicals, respectively (reactions 3 and 4). On the basis of the relative concentrations of DMSO and NO_2^- and their published rate constants for the $^{\bullet}OH$ reaction,[37] the yield of $^{\bullet}NO_2$ and $^{\bullet}CH_3$ is calculated to be 92% and 8%, respectively, independent of $[O_2]$. Under 20% O_2, the methyl radicals are converted to methyl peroxy radicals (~95%, reaction 6), as calculated from the relative concentrations of O_2 and **I** and their published rate constants for reaction with methyl radicals;[37] **II** formation then represents the sum of $^{\bullet}NO_2$ and $^{\bullet}CH_3$ formation (reactions 8 and 9; Figure 5A). With decreasing $[O_2]$, **II** formation decreases, while the methoxylamine (**VI**) formation increases due to greater reaction of **I** with the methyl radical (reaction 7, Figure 5B, and Scheme 1); under complete deoxygenation, **II** decreases by 10%, in good agreement with the calculated percentage of methyl radicals generated under these conditions (8%, see above). As shown in the Supporting Information, the decrease in the yield of **II** and the concomitant increase in the yield of **VI** with decreasing $[O_2]$ are in good agreement with those calculated based on known rate constants (reactions 1−9 and Scheme 1).

Although the $[O_2]/[\mathbf{I}]$ ratio was altered by decreasing the $[O_2]$ in the above example, an increase in [**I**] could also have been employed. It should be further noted that this example is particularly challenging in that a small amount of peroxyl radical was detected over a very high background of $^{\bullet}NO_2$.

Thermal and Photochemical Stability of I and II. Both **I** and **II** were stable for 12 or more hours in aqueous solution over a broad range of conditions, including pH ranging from 4 to 10 and temperatures up to 50 °C, as determined by UV−vis, fluorescence, and EPR spectroscopies and by chromatographic analysis. However, irradiation of **I** or **II** with high-intensity polychromatic light led to observable photodegradation (15%) of **I** and significant photodegradation (60%) of **II** over the course of 60 min, as determined by UV−vis. These results indicate that while **I** can be employed in thermal systems, it will not be suitable generally for photochemical studies. In contrast, 3-ap and the 3-ap oxidation product were stable at pH 6−8 under either thermal (up to 38.5 °C) or irradiation conditions over time scales extending to 90 min as established by UV−vis and HPLC. Thus, **I** was employed to determine peroxyl radicals in thermal systems, while 3-ap, followed by derivatization of the product to form **II**, was used in photochemical studies (see below).

Linearity, Precision, and Detection Limit. Employing the AAPH system, the concentration of **II** was calibrated by comparing the loss of nitroxide as measured by EPR with the increase in the fluorescence peak area in HPLC chromatograms (Figure 3 inset). Once product concentrations in the micromolar range were established, a calibration curve in the nanomolar range, where EPR determinations were not possible, was generated by serial dilution of **II**. Steady-state emission spectra were calibrated in the same fashion (Figure 3 inset). Chromatographic peak areas increased linearly over the concentration range of 5−7500 nM (n = 9) with an R^2 value of 0.998, and the y intercept was not significantly different from zero. Employing direct fluorometric detection, the linear range was from 0.66 to 6.2 μM with an R^2 value of 0.997. The precision of the HPLC analysis method was determined from the reproducibility of five HPLC injections of identical samples under the same experimental conditions over a period of 7 days at concentrations in the nanomolar range (10−50 nM). The maximum RSD was 10.6% for HPLC separation with fluorescence detection. In a similar fashion, the maximum RSD for direct fluorometric detection method was 9.2%. Defining the detection limit as twice the standard error of the intercept obtained from linear regressions of calibration curves of **II**, with concentrations ranging from 5 to 240 nM (6 points; HPLC separation with fluorescence detection) and from 0.66 to 6.2 μM (6 points; direct fluorometry), we estimate values of ~3 nM for the HPLC analysis (125 μL injection volume) and ~0.35 μM for direct fluorometric detection.

Preliminary Applications. Employing **I**, peroxyl radical formation was detected in an aqueous dispersion of soybean PC

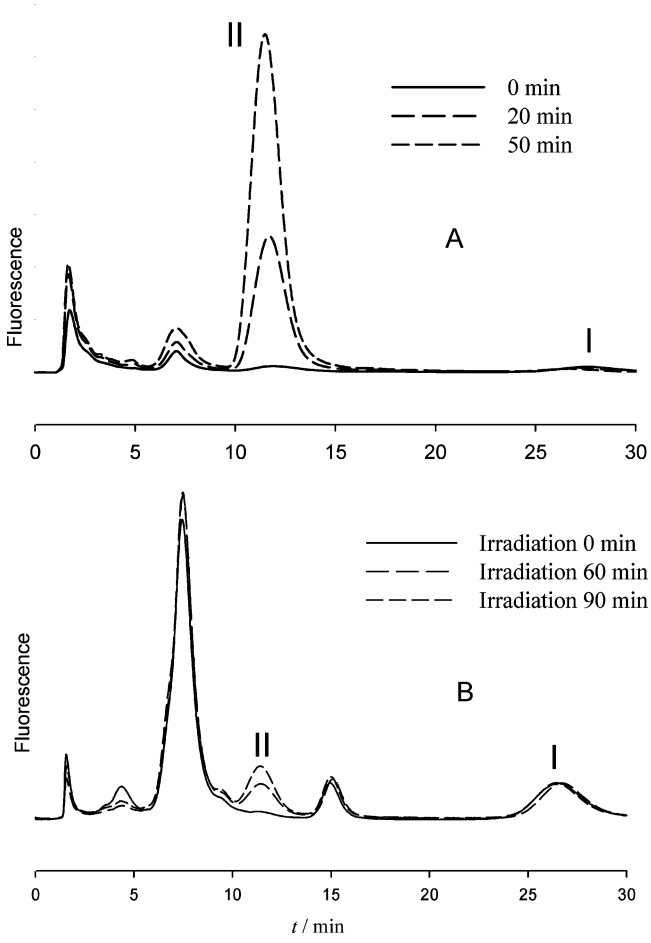

Figure 6. Application of **I** and 3-ap. (Panel A) Formation of **II** in soybean PC liposome system incubated at 50 °C in the presence of 1 mM AIBN. $[O_2] = 180\ \mu M$, $[\mathbf{I}] = 28.4\ \mu M$, and [PC] = 100 mM. HPLC conditions were the same as in Figure 3. (Panel B) Peroxyl radical detection in irradiated tap water using 3-ap as the probe followed by derivatization with fluorescamine after irradiation. $[\mathbf{I}] = 10\ \mu M$. Irradiation conditions are as described in the Experimental Section.

lipsomes, a common model for cell membranes.[34−36] A water-insoluble azo compound, 2,2′-azo-bis-isobutyronitrile (AIBN), was used to initiate autoxidation of the polyunsaturated fatty acids within the PC liposomes via incubation at 50 °C under air. Analysis of the reaction mixture by HPLC showed that **II** increased with increasing incubation time (Figure 6A), from 2.9 μM at 20 min to 7.4 μM by 50 min. In the absence of the radical initiator (AIBN), **II** was not detected (data not shown).

Photochemical formation of peroxyl radicals was observed upon irradiation of tap water with polychromatic light; in this case, 3-ap was used with the product immediately derivatized with fluorescamine at pH 8.1 after irradiation (Figure 6B). Formation of **II** increased with increasing irradiation time from 180 nM at 60 min to 250 nM at 90 min. **II** was not formed when Milli-Q water was irradiated in the presence of 3-ap nor when tap water was irradiated in the absence of 3-ap. To test for the presence of other oxidants, tap water was irradiated under anaerobic conditions and the generation of alkoxylamine products was determined chromatographically. Consistent with prior work,[9] acetyl and methyl alkoxylamines were identified as the major products, with their total concentration increasing from 130 nM at 60 min to 200 nM at 90 min. This significantly lower yield of the alkoxylamine products relative to **II** suggests the presence of an additional oxidant or oxidants.

CONCLUDING REMARKS

The irreversible reaction of **I** and 3-ap with peroxyl radicals and other radical oxidants has two major consequences. First, because the reaction is stoichiometric (Figure 1A,B) and the product of these reactions is reasonably stable (**II**), highly sensitive, quantitative measurements of the rates of oxidant formation can be obtained (Figures 1−5 and Figures S2 and S3 in the Supporting Information). Second, because the oxoammonium cation is not stable and rapidly decays to another species (Figures 3 and 4), possible secondary oxidation reactions by the cation should be eliminated, thus precluding the formation of spurious secondary oxidation products.[39,45]

One disadvantage of this approach is that the peroxy radicals, unlike most carbon-centered radicals, do not form stable adducts with nitroxides (Scheme 1, Figures 1−3, and Figure S3 in the Supporting Information),[39−42] and thus information on the structure of the peroxyl radical is lost. However, as shown here, lower concentrations of O_2 (or higher concentrations of **I**) can be employed to allow interception of the carbon-centered radicals by **I** prior to O_2 reaction, with the stable alkoxyamine products then generated providing information on structure (Scheme 1 and Figure 5).[27,28,32,33] Further, changing the $[O_2]/[\mathbf{I}]$ ratio can allow discrimination between peroxyl radicals and other one-electron oxidants (Figure 5).

Another potential problem is the reduction of **I** to the hydroxylamine by certain compounds[18,27,28] and by cells[27−29] that also results in enhanced fluorescence. Although this problem should be alleviated to some extent by the use of low concentrations of **I**, it will likely limit the direct fluorometric detection in some cases. However, even in these cases, HPLC analysis will still allow a clear discrimination among products (Figure 5)[9] and thus the selective detection of these radicals.

ACKNOWLEDGMENT

This work was supported by a Graduate Research Board Award from the University of Maryland to N.V.B. and in part by grants from the ONR and the NSF (N.V.B.). We thank Prof. M. Al-Sheikhly and Ms. Alia Weaver of the University of Maryland for access to and assistance with the ^{60}Co source. We thank Dr. Elizabeth Kujawinski and Melissa Soule for the FTICR mass spectra measurements.

SUPPORTING INFORMATION AVAILABLE

The product formation of the **I** reaction with methyl peroxyl radical; the structure analysis of **II** and **V** by FTICR MS and NMR, and the product formation of $^{\bullet}NO_2$ and $CO_3^{\bullet-}$ radical reaction with **I**. This material is available free of charge via the Internet at http://pubs.acs.org.

Received for review June 24, 2009. Accepted August 27, 2009.

AC901374M

(45) Lardinois, O.; Maltby, D.; Medzihradszky, K.; Montellano, P. R.; Tomer, K.; Mason, R.; Deterding, L. *Chem. Res. Toxicol.* **2009**, *22* (6), 1034–1049.